Thomas-Fermi theory of screening of a point-charge impurity in an insulator: Nonzero temperature

J. Oliva
Department of Physics-Astronomy, California State University, Long Beach, California 90840
*and Department of Physics, California State University, San Bernardino, California 92407**
(Received 25 September 1989)

The nonzero-temperature electrostatic screening of a point charge embedded in an insulator is analyzed in a model study based on the two-band version of the Thomas-Fermi (TF) theory. The form for the screened potential at large distance from the impurity is obtained in terms of quadratures. This asymptotic expression is then evaluated in closed analytic form in the limit of low temperature. Numerical solution of the exact (nonlinear) TF equation is also carried out. Numerical results are given for the spatial dielectric function (equivalent to the potential) showing its dependence on distance from the impurity, temperature, impurity charge strength, and band gap. Results here for nonzero temperature are compared with results for zero temperature obtained earlier within the same TF framework.

I. INTRODUCTION

We present results of an application of the two-band generalization of the Thomas-Fermi (TF) method in a model study of the electrostatic screening response of a pure insulator and/or semiconductor to an embedded point charge at nonzero temperature. The two-band TF generalization was earlier examined by Brooks and Herring[1] and Dingle[2] in the context of screening of a point charge in extrinsic semiconductors with carriers in both bands. This approach is also used in the now standard analysis of the *p-n* junction.[3] More recently the method was applied to the present problem but at zero temperature by the author.[4,5] (Here the mathematical analysis is somewhat different than at nonzero temperature.) The basic idea of this generalized TF method is to determine the function giving the charge density ρ in terms of the electrostatic potential φ (a main step in TF theory) using a local band structure having two parabolic bands separated by a gap (appropriate for an insulator) rather than using the usual single parabolic local band.

The two-band TF approach leads to a nonlinear differential equation for φ (the TF equation) which is generally only numerically solvable. Working within the intrinsic case of interest here, we first consider the TF equation when linearized in φ (e.g., for large distance from the impurity); the basic form of φ can then be found in terms of quadratures. With the additional assumption of temperature T low compared to the gap and valence bandwidth we find a closed analytic form for the general solution for φ. We then present numerical results for the original exact (nonlinear) TF equation, focusing on the spatial dielectric function $\bar{\epsilon}(r)$ (equivalent to the potential) for arbitrary distance r from the impurity.

A number of studies of free-carrier screening of a charged point impurity in an insulator and/or semiconductor at nonzero T have been reported: Among the earliest are those of both Brooks and Herring[1] and Dingle[2] (as noted) and also of Mansfield[6] who all used a linearized TF approach in analyzing this problem in extrinsic semiconductors. (Mansfield considered carriers in only one band.) The screened potential in these approaches was found to be of the Yukawa form. More recent studies going beyond, but often based on, these earlier works have been carried out: The effect on the screening due to spatial variation of the valence-electron dielectric response has been considered within the linearized TF approach by Csavinszky[7] and within a nonzero T nonlocal linear response theory by Resta.[8] Nonlinear screening effects (i.e., going beyond the linearized TF approach of Refs. 1, 2, and 6) were examined by Csavinszky[8] and Adawi[10] (both keeping terms up to quadratic in the potential). A variational treatment allowing, in principle, for account of terms of all orders in the potential was developed by Csavinszky.[11] Nonlinear studies including a dispersive valence-electron dielectric response have been carried out by Brownstein[12] (variational) and Meyer[13] (numerical). (Both of these works note and incorporate improvements made subsequent to the underlying study of Ref. 7.) The effect of polarization of the screening cloud by an outside electron was considered within linear response by Takimoto.[14] Hall[15] then considered the form of the potential starting with Takimoto's work and using an extended mathematical analysis. Another approach to the screening response, pursued by Stern,[16] Agarwal and Singh,[17] and Patterson and Lehoczky[18] centers on the determination of the screening length in a Yukawa form potential by the use of the Friedel sum rule (phase shifts are analyzed in a low-order Born approximation). For a recent, more complete review of activity in the above overall area see Chattopadhyay and Queisser.[19]

We should note that the above nonzero-T point-charge-screening studies (as well as those referred to in Ref. 19) predominantly focus on the extrinsic case, most often where there are carriers in only one band, and generally do not directly carry over to the intrinsic case.[20]

On the other hand, these studies could be adapted to and are in any event relevant to this latter case. As noted, the present work is concerned with screening by free carriers in the intrinsic case. Again, we furthermore use a numerical treatment of the exact (i.e., fully nonlinear) TF equation. The screening is analyzed at arbitrary temperature. The treatment here, also of the linearized TF theory, is compared to the linearized TF study of Dingle[2] (case of carriers in both bands) which, though primarily focusing on extrinsic effects in the screening, also implicitly includes (but does not discuss) the intrinsic case. We note that Stern[16] obtains essentially the same result as Dingle, though from outside the TF framework (see above); again the intrinsic case is implicitly included but not discussed.

The paper is organized as follows: Section II presents details of the overall model. Section III gives an extended discussion of the two-band generalization of the TF method. Next the nonzero-temperature TF equation is derived and the general form for φ for small φ is analyzed. The low-T limiting form of this small φ solution for φ is then developed. Section IV discusses the numerical procedure for solving the TF equation. Numerical results for $\bar{\epsilon}(r)$ are then presented in Sec. V. We discuss the effect on $\bar{\epsilon}(r)$ of varying the temperature, the impurity charge strength, and the energy gap. Finally Sec. VI contains a conclusion.

II. MODEL

The insulator is modeled in a simple way: We have a local band structure varying with position and consisting of two parabolic bands separated by a direct energy gap E_g (see Fig. 1). The valence band has width B while the conduction band has infinite width. The electron effective masses of conduction and valence bands are denoted by m_c and m_v, respectively (note $m_v<0$). Each Bloch state in each of the above bands can accommodate two electrons (spin up, spin down) and is thus at least doubly degenerate. We allow for additional degeneracy d_c and d_v in Bloch states in conduction and valence bands, respectively. Thus, the overall degeneracies of conduction and valence bands are $2d_c$ and $2d_v$, respectively (the factor 2 again is due to spin degeneracy).

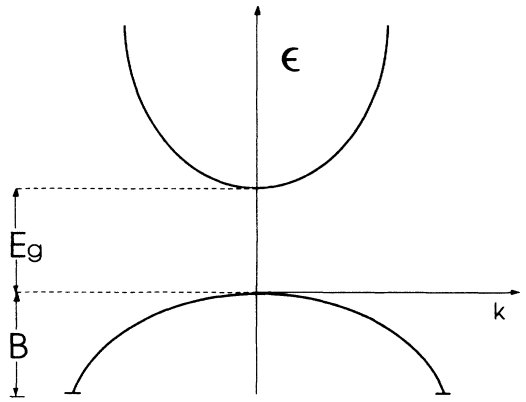

FIG. 1. Form of band structure in insulator model: both valence and conduction bands are parabolic. The valence band has width B and the conduction band has infinite width.

We assume that the local band structure is shifted "rigidly" in energy depending on the local value of the potential $\varphi(r)$: This potential is assumed constant for each small local region of the system and is nominally assumed to vary slowly from region to region. (This is the usual slow variation assumption of TF theory.) For very large distances, far removed from the electron-density perturbation near the impurity, the local band structure is essentially r independent. We then take the zero of energy E to be at the maximum of the asymptotic local valence band. Note that here $\varphi(r)$ is determined by the charge density which, in turn, depends on $\varphi(r)$, i.e., $\varphi(r)$ is self-consistent in this sense.

As we approach a positive impurity, the potential will be nonzero and increasingly positive and thus the local band structure "sweeps" downward in energy (see Fig. 2). Now the Fermi level μ is determined by the asymptotic band structure: For T approaching zero μ tends to $E_g/2$. At nonzero temperature, electron occupation of the asymptotic conduction band along with electron depletion of the asymptotic valence band occurs. Except at low temperatures the Fermi level deviates appreciably from the gap midpoint energy $E_g/2$. Now, as the local band structure sweeps downward in energy in moving to-

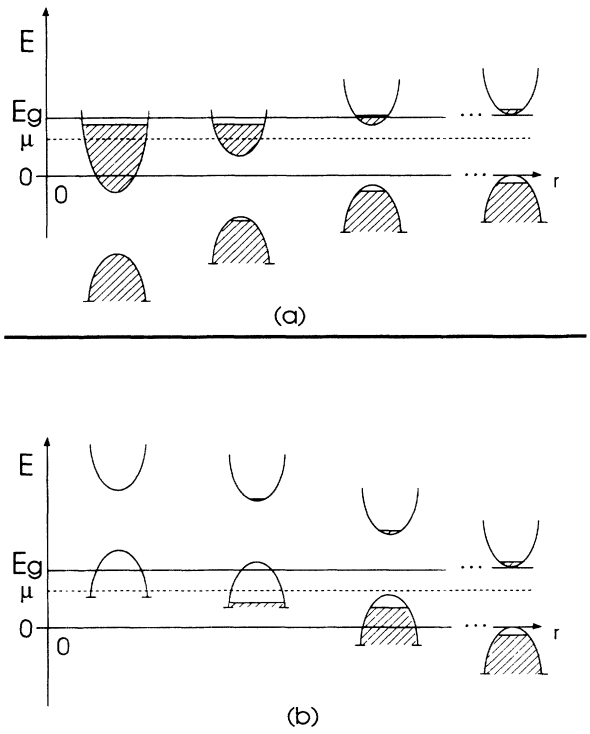

FIG. 2. Qualitative behavior of local band structure near (a) positive and (b) negative impurity at nonzero temperature. As distance to impurity increases, the local upper valence-band edge tends to $E=0$. Fermi level μ is set by asymptotic local band structure and temperature. The shading (absence of shading) in the local conduction (valence) band give a schematic indication of roughly where the electron (hole) occupation is appreciable at a nonzero temperature.

ward the positive impurity, the electron occupation of the local conduction and valence bands increases. This is most clear very near the impurity where the band edges are much lower than the level of μ. For $T\rightarrow 0$ indeed all states in the local bands are filled up to the level $\mu=E_g/2$ as seen earlier.[21] For close proximity to the impurity this level will, in fact, pass somewhere through the local conduction band.

As we approach a negative impurity, the local band structure now "sweeps" upward in energy since the potential is now increasingly negative for decreasing r (see Fig. 2). The effect of moving closer to the impurity is to ultimately reduce electron occupation in both local conduction and valence bands. This follows since the local bands are becoming higher in energy relative to the fixed Fermi level as $r\rightarrow 0$. The depletion of electrons is analogous to the type encountered in the zero-temperature analysis.[5] There valence-band depletion begins when the "sweeping" valence-band maximum first crosses the Fermi level at $E_g/2$; the conduction band remains empty. We lastly note that our model incorporates a positive, uniform, and fixed background charge density which precisely cancels the uniform asymptotic charge density of the electrons.

III. THOMAS-FERMI ANALYSIS

We first present an explication of the two-band TF generalization (see above). In the two-band TF analysis, we will be concerned with electron occupation of both local bands as described and ultimately with the potential $\varphi(r)$ [or equivalently the spatial dielectric function $\bar{\epsilon}(r)$]. As noted we will nominally make the slow potential variation assumption of TF. We will then, for semiquantitative purposes, apply the TF results to the rapid density variation region in the near vicinity of the impurity. This is generally done in the TF analysis of, e.g., the standard problem of a point charge in a metal.

The two-band generalized TF equation for $\varphi(r)$, as with the usual TF equation, is Poisson's equation with the total charge density written explicitly as a function of the potential

$$\nabla^2\varphi=-4\pi\rho(\varphi) \ . \tag{1}$$

Now in the two-band TF case the determination of the function $\rho[\varphi(r)]$ is based not only on the principle of constancy of the chemical potential (for a system in diffusive equilibrium), as with the usual TF theory, but also (as noted) on the use of a two-band local band structure for the electrons. The function $\rho[\varphi(r)]$ has two contributions (one from each band), each involving integration of a local Fermi factor (incorporating the potential) times the single-particle density of states for the (parabolic) band involved.

We note that here the boundary conditions on $\varphi(r)$ are given by

$$\lim_{r\rightarrow 0} r\varphi(r)=Ze \ , \tag{2a}$$

$$\lim_{r\rightarrow\infty}\varphi(r)=0 \ , \tag{2b}$$

where Ze is the impurity charge (with e being the magnitude of the electron charge and with Z either positive or negative).

The total charge density which enters Eq. (1) is taken here as an external charge density, associated with the impurity, background, and electrons in the local valence and conduction bands. Thus, in this initial, semiquantitative model study we choose not to include in our main calculation the effect of dielectric polarization.[22] Rather, we focus here on local band filling and nonzero-T effects. We do, however, discuss below the modification of our results (for some aspects quantitatively) upon inclusion of this dielectric polarization effect. Further examination of the inclusion of this effect via the use of a spatially varying dielectric constant is being considered.[23]

We thus begin to develop the two-band generalized TF equation by considering the relation between the conduction- and valence-band electron densities and the potential. We first establish the value of the Fermi energy μ. Now the electron charge density for the valence band for $r\rightarrow\infty$ and $T=0$ is denoted by $-en_0$. This charge density arises purely from the filled local valence band (with the conduction band empty). Thus, n_0 is the number of local valence-band states per unit volume. The charge density of the uniform background is then $+en_0$. Now, as T increases or for finite r, the local conduction band will have acquired some occupation while the local valence band will be depleted to some extent. In general, we denote the density of electrons in the local conduction band at distance r (and at arbitrary T) by $\delta n_c(r)$. We denote the density of electrons in the local valence band at distance r (and at arbitrary T) by $n_v(r)$. We then have

$$n_v(r)=n_0+\delta n_v(r) \ , \tag{3}$$

where $\delta n_v(r)$ is the corresponding local change in valence-band electron density from the filled value n_0. Note $\delta n_v(r)$ is necessarily negative.

Now the total charge density ρ for $r\neq 0$, including conduction band, valence band, and background contributions is

$$\rho(r)=-e[\delta n_c(r)+n_v(r)-n_0] \quad (r\neq 0) \ . \tag{4}$$

Using Eq. (3) in Eq. (4) we then get

$$\rho(r)=-e[\delta n_c(r)+\delta n_v(r)], \quad r\neq 0 \ . \tag{5}$$

Note that $\delta n_c(r)\neq-\delta n_v(r)$ in general. This is due to the fact that the local bands shift relative to the *fixed* chemical potential as r varies.

At nonzero T we then have the well-known forms for the quantities $\delta n_c(r)$ and $\delta n_v(r)$ in the presence of an electrostatic potential.[24]

$$\delta n_c(r)=\int_{E_g}^{\infty}\frac{\rho_c(\varepsilon)d\varepsilon}{e^{\beta[\varepsilon-e\varphi(r)-\mu]}+1} \ , \tag{6a}$$

$$\delta n_v(r)=-\int_{-B}^{0}\frac{\rho_v(\varepsilon)d\varepsilon}{e^{\beta[\mu-\varepsilon+e\varphi(r)]}+1} \ . \tag{6b}$$

Here $\beta\equiv 1/k_BT$ where k_B is Boltzmann's constant, and

the (parabolic) band single-particle density of states per unit volume ρ_c and ρ_v are given by[24]

$$\rho_c(\varepsilon)=\frac{d_c}{2\pi^2}\left[\frac{2m_c}{\hbar^2}\right]^{3/2}(\varepsilon-E_g)^{1/2},\quad \varepsilon\geq E_g\ , \tag{7a}$$

$$\rho_v(\varepsilon)=\frac{d_v}{2\pi^2}\left[\frac{-2m_v}{\hbar^2}\right]^{3/2}(-\varepsilon)^{1/2}\ ,\quad -B\leq\varepsilon\leq 0\ . \tag{7b}$$

Note the minus sign in Eq. (6b) since δn_v is always a decreasing change in density as discussed above. Note that the location of the zero of the energy ε is at the *shifted*, i.e., local valence-band maximum.

We now determine the Fermi energy by letting $r\to\infty$ which implies [Eq. (2b)] $\varphi(r)\to 0$ in Eqs. (6). At infinity the total charge density ρ vanishes as noted. Using this and Eqs. (6) (with $\varphi=0$) in Eq. (5) we obtain the equation which determines μ:

$$\int_{E_g}^{\infty}\frac{\rho_c(\varepsilon)d\varepsilon}{e^{\beta(\varepsilon-\mu)}+1}=\int_{-B}^{0}\frac{\rho_v(\varepsilon)d\varepsilon}{e^{\beta(\mu-\varepsilon)}+1}\ . \tag{8}$$

The determination of μ is generally carried out numerically. At very low temperatures ($\beta E_g\gg 1$, $\beta B\gg 1$) we find the analytic result for μ:[25]

$$\mu=\tfrac{1}{2}E_g+\tfrac{1}{2}k_BT\left[\ln\left[\frac{d_v}{d_c}\right]+\tfrac{3}{2}\ln\left[\frac{|m_v|}{m_c}\right]\right]\qquad(\beta E_g\gg 1,\ \beta B\gg 1)\ . \tag{9}$$

We use Eqs. (6) and (7) in Eq. (5) to find the net charge density for $r\neq 0$ as a function of $\varphi(r)$:

$$\rho(r)=\rho(\varphi(r))=\frac{\sqrt{2}e}{\pi^2\hbar^3}\left[-d_cm_c^{3/2}\int_{E_g}^{\infty}\frac{(\varepsilon-E_g)^{1/2}d\varepsilon}{e^{\beta[\varepsilon-e\varphi(r)-\mu]}+1}+d_v(-m_v)^{3/2}\int_{-B}^{0}\frac{(-\varepsilon)^{1/2}d\varepsilon}{e^{\beta[\mu-\varepsilon+e\varphi(r)]}+1}\right]\quad(r\neq 0)\ . \tag{10}$$

Upon using Eq. (10) in Poisson's equation, Eq. (1), we find

$$\nabla^2(e\varphi(r))=c_c\int_{E_g}^{\infty}\frac{(\varepsilon-E_g)^{1/2}d\varepsilon}{e^{\beta[\varepsilon-e\varphi(r)-\mu]}+1}-c_v\int_{-B}^{0}\frac{(-\varepsilon)^{1/2}d\varepsilon}{e^{\beta[\mu-\varepsilon+e\varphi(r)]}+1},\quad r\neq 0\ , \tag{11}$$

where

$$c_c=\frac{2d_ce^2}{\pi}\left[\frac{2m_c}{\hbar^2}\right]^{3/2}, \tag{12a}$$

$$c_v=\frac{2d_ve^2}{\pi}\left[\frac{-2m_v}{\hbar^2}\right]^{3/2}. \tag{12b}$$

The impurity contribution to the charge density, which is $\sim\delta^3(r)$, is not evident in Eq. (11) because of the restriction $r\neq 0$. Its effect comes into the solution of Eq. (11) via the boundary condition Eq. (2a). Equation (11) is then the two-band generalized TF equation for $\varphi(r)$ for the above insulator model at nonzero T. Introducing $p(r)$ defined via

$$e\varphi(r)=\frac{p(r)}{r} \tag{13}$$

and using

$$\nabla^2\left[\frac{p}{r}\right]=\frac{1}{r}\frac{d^2p}{dr^2}\ , \tag{14}$$

we then have the TF equation for $p(r)$:[26]

$$\frac{1}{r}\frac{d^2p(r)}{dr^2}=c_c\int_{E_g}^{\infty}\frac{(\varepsilon-E_g)^{1/2}d\varepsilon}{e^{\beta[\varepsilon-p(r)/r-\mu]}+1}-c_v\int_{-B}^{0}\frac{(-\varepsilon)^{1/2}d\varepsilon}{e^{\beta[\mu-\varepsilon+p(r)/r]}+1},\quad r\neq 0\ . \tag{15}$$

In general, this equation must be solved numerically. We can, however, obtain the solution for $p(r)$ for the case of small p/r in terms of quadratures. This corresponds here to the large-r regime. We begin by expanding the right-hand side of Eq. (15) in powers of p/r. Keeping terms to first order in p/r we are led to the following:

$$\frac{1}{r}\frac{d^2p(r)}{dr^2}=c_c\int_{E_g}^{\infty}\frac{(\varepsilon-E_g)^{1/2}d\varepsilon}{e^{\beta(\varepsilon-\mu)}+1}-c_v\int_{-B}^{0}\frac{(-\varepsilon)^{1/2}d\varepsilon}{e^{\beta(\mu-\varepsilon)}+1}+\frac{\beta}{4}\left[c_c\int_{E_g}^{\infty}\frac{(\varepsilon-E_g)^{1/2}d\varepsilon}{\cosh^2[\beta(\varepsilon-\mu)/2]}+c_v\int_{-B}^{0}\frac{(-\varepsilon)^{1/2}d\varepsilon}{\cosh^2[\beta(\varepsilon-\mu)/2]}\right]\frac{p(r)}{r},\quad r\neq 0\ . \tag{16}$$

Now the first two terms in the right-hand side of Eq. (16) precisely cancel by the condition defining the Fermi level μ [see Eq. (8)]. We then define the constant K as the square root of the coefficient in the term linear in p/r on the right-hand side of Eq. (16):

$$K \equiv \frac{\beta^{1/2}}{2}\left[c_c \int_{E_g}^{\infty} \frac{(\varepsilon - E_g)^{1/2} d\varepsilon}{\cosh^2[\beta(\varepsilon-\mu)/2]} + c_v \int_{-B}^{0} \frac{(-\varepsilon)^{1/2} d\varepsilon}{\cosh^2[\beta(\varepsilon-\mu)/2]}\right]^{1/2} . \tag{17}$$

Then Eq. (16) becomes

$$\frac{d^2 p(r)}{dr^2} - K^2 p(r) = 0, \quad \frac{p}{r} \to 0 , \tag{18}$$

which has the following general solution:

$$p(r) = A e^{-Kr} + A' e^{Kr} , \tag{19}$$

where A and A' are constants. Naturally on physical grounds we keep only the decaying solution. Thus,

$$p(r) = A e^{-Kr}, \quad \frac{p}{r} \to 0 , \tag{20}$$

or

$$\varphi(r) = \overline{A} \frac{e^{-Kr}}{r}, \quad r \to \infty , \tag{21}$$

where $\overline{A} = A/e$.

We briefly note the modification of the large-r solution for φ on the inclusion of the dielectric polarization effects. As implied in Ref. 22, at large r, $p(r)$ would satisfy a modified Eq. (18) now with a factor of the static dielectric constant κ_0 multiplying the first term on the left-hand side. This gives, for the modified potential φ_1,

$$\varphi_1(r) = \overline{A}_1 \frac{e^{-K_1 r}}{r}, \quad r \to \infty , \tag{22}$$

where $\overline{A}_1$ is a constant, and where

$$K_1 = \frac{K}{\kappa_0^{1/2}} . \tag{23}$$

Note that $\overline{A}_1$ will manifest the r-dependent polarization effects occurring at smaller r.

The result for K_1 [Eq. (23)] derived for the intrinsic case in the linearized approximation is nearly the same as the results implied in the work of Dingle[2] (for the extrinsic case with carriers in both bands) and of Stern.[16] [For Dingle see his $1/R$ —his Eq. (23)—using his Eq. (24) and take the intrinsic limit; for Stern see his $1/L$ –his Eq. (6)–and determine his relative Fermi energies E_{fi} according to the level of the intrinsic chemical potential defined via our Eq. (8).] Our result for K_1 differs from theirs in that we treat the finite-valence-bandwidth case whereas they set $B = \infty$. Further, Dingle does not include arbitrary degeneracy factors (present in c_c and c_v here), he sets $d_c = d_v = 1$. [Note that Dingle and Stern use the linearized (from a TF viewpoint) solution for all r and thus determine $\overline{A}_1 = Ze/\kappa_0$ ($Z = 1$ in Dingle) from their $r \to 0$ boundary condition.]

Thus, the asymptotic behavior of φ is of the "Yukawa" form with a basic inverse r times exponential decay. This metallic, long-range perfect screening form contrasts with results found earlier using the same TF analysis but at zero temperature.[4,5] There we found the asymptotic form $\varphi \sim 1/r$, i.e., a nonmetallic, long-range imperfect screening form. Thus, there is a major qualitative difference between the $T = 0$ and $T \neq 0$ forms of the potential. Note in Eq. (21) that the temperature dependence and the band-structure parameter dependence (i.e., dependence on E_g, B, m_c, m_v, d_c, and d_v) of the asymptotic potential comes in through K *and* $\overline{A}$.

We naturally expect that at temperatures very low compared to the gap, the decay length K^{-1} in Eq. (21) will be very large compared to a typical metallic case, i.e., the system is then trying to behave as the $T = 0$ insulator. For temperatures comparable to the gap, however, K^{-1} may be relatively small in many cases (see Sec. V). It is, in fact, to be expected that the qualitative distinction between insulator and metal with respect to long-range screening will disappear at nonzero temperature. Indeed, in the insulator, a Debye-like shielding effect occurs at low temperatures involving the low density gas of thermally excited electrons and holes which is in the classical regime. This will give rise to long-range perfect screening independent of local band-shift effects.

We now consider the leading order low-temperature form of K. We assume $\beta E_g \gg 1$ and $\beta B \gg 1$ and consider first the term I_1 in K^2 from Eq. (17):

$$I_1 \equiv \frac{c_c \beta}{4} \int_{E_g}^{\infty} \frac{(\varepsilon - E_g)^{1/2} d\varepsilon}{\cosh^2[\beta(\varepsilon-\mu)/2]}$$
$$\approx c_c \beta \int_{E_g}^{\infty} (\varepsilon - E_g)^{1/2} e^{-\beta(\varepsilon - E_g/2)} d\varepsilon \quad (\beta E_g \gg 1) . \tag{24}$$

We have used $\mu \to E_g/2$ in this limit. With a change of variable $v = \beta(\varepsilon - E_g)$ we see that the integral in Eq. (24) is $\sim \Gamma(\frac{3}{2}) = \pi^{1/2}/2$. We find

$$I_1 \approx \frac{\pi^{1/2}}{2} \frac{c_c}{\beta^{1/2}} e^{-\beta E_g/2}, \quad \beta E_g \gg 1 . \tag{25}$$

Next the second term I_2 in K^2 from Eq. (17) is considered:

$$I_2 \equiv \frac{c_v \beta}{4} \int_{-B}^{0} \frac{(-\epsilon)^{1/2} d\varepsilon}{\cosh^2[\beta(\varepsilon-\mu)/2]}$$
$$\approx c_v \beta \int_{-B}^{0} (-\varepsilon)^{1/2} e^{\beta(\varepsilon - E_g/2)} d\varepsilon, \quad \beta E_g \gg 1 . \tag{26}$$

Upon replacing the integration limit $-B$ by $-\infty$ (i.e., using $\beta B \gg 1$) and changing variables to $v = -\beta\varepsilon$, the integral in Eq. (26) is seen to be $\sim \Gamma(\frac{3}{2})$ also. We find

$$I_2 \approx \frac{\pi^{1/2}}{2} \frac{c_v}{\beta^{1/2}} e^{-\beta E_g/2}, \quad \beta E_g \gg 1, \ \beta B \gg 1 . \tag{27}$$

Using Eqs. (25) and (27) in Eq. (17) we have the leading low-temperature form for K:

$$K \approx \frac{\pi^{1/4}}{2^{1/2}} \frac{(c_c + c_v)^{1/2}}{\beta^{1/4}} e^{-\beta E_g/4}, \quad \beta E_g \gg 1, \ \beta B \gg 1 \ . \quad (28)$$

Again, the effect of including dielectric polarization effects here would be to divide the right-hand side of Eq. (28) by $\kappa_0^{1/2}$. Thus, for $T \to 0$, $K \to 0$ as expected and we tend to recover the large-r $\varphi(r) \sim 1/r$ behavior for increasingly larger r. The now weaker exponential decay factor in φ will, of course, be apparent for $r \gg K^{-1}$.

We consider the formal behavior of φ for $T \to \infty$ (this is academic as the band structure will change at melting at finite T). For $T \to \infty$ the valence band may be ignored and we have a limiting classical free-electron gas for which $e^{\beta\mu} \to 0$. Equation (17) then gives $K \to 0$ in this limit. Thus, φ then has such a large decay length K^{-1} that for practical purposes it varies for large r (but $r \ll K^{-1}$) as $\sim 1/r$. In fact, it should be given by $\varphi \approx Ze/r$ for the whole range $r \ll K^{-1}$. This follows physically as the screening cloud vanishes as $T \to \infty$.

IV. SOLUTION OF THE TF EQUATION

We discuss the numerical procedure for solving the TF equation for $p(r)$, Eq. (15). As noted above, we first solve for the Fermi level μ for the given band structure and temperature by examining the large-r region [see Eq. (8) and discussion thereof]. We then consider the form of the large-r solution for $p(r)$, Eq. (20); the constant K is found using a direct numerical integration in Eq. (17). The constant A is undetermined at this point. We next return to the full form of the TF equation (15) for arbitrary r. To avoid undue computation time evaluating integrals in solving Eq. (15) numerically, we initially develop a spline fit for the right-hand side of Eq. (15) for a wide range of p/r.

We then start integrating Eq. (15) outward from the origin using the boundary value

$$p(0) = Ze^2 \quad (29)$$

which follows from the small-r form for φ [Eq. (2a)]. We integrate out with a guess for the initial slope such that p/r decreases for increasing r. We then choose a trial, "large" value of r which we denote by r_x. At this r_x we inquire whether the logarithmic derivative of the numerically integrated form, L_1, agrees with the logarithmic derivative of the analytic large-r form of φ [Eq. (20)], L_2. This latter form is given by

$$L_2 = -K \ . \quad (30)$$

We try to attain a match by varying the initial slope of the numerical solution until we thus satisfy

$$L_1 = -K, \quad r = r_x \ . \quad (31)$$

[Our condition for a match was agreement in Eq. (31) to within one part in $\sim 10^3$).]

If we do find an initial slope giving a solution p/r whose L_1 satisfies Eq. (31), we then inquire as to whether the value of p/r at r_x (from the numerical procedure) is sufficiently small that the truncation to first order in p/r in Eq. (16) is justified at the given r_x [this would justify our use of Eq. (20) for $r \geq r_x$]. To do this we check that in Eq. (16) each of the two linear terms evaluated at $p(r)/r = p(r_x)/r_x$ is small in magnitude compared to the magnitude of the corresponding zeroth-order term. (As noted, the two zeroth-order terms there cancel.) If the ratio of linear to zeroth-order terms is small (we use $\sim 10^{-3}$) we are then most likely justified in using the first-order truncated Eq. (16), rendering Eq. (20) valid. In this case we have a solution for all r: for $r < r_x$ we have the numerical solution and for $r > r_x$ we have the analytic form Eq. (20); at $r = r_x$ the logarithmic derivatives are continuous and the prefactor A in Eq. (20) can be deduced from boundary matching of the numerical and analytic forms for p at $r = r_x$.

If, on the other hand, the first-order term in Eq. (16) is too large for the initial guess r_x, we repeat the whole process but start with a suitable larger guess for r_x. We continue iterating over r_x until we find a solution which satisfies the logarithmic derivative continuity requirement and for which r_x is sufficiently large to justify the truncation in Eq. (16). We, thus, are doing a double search: we vary the initial slope and r_x until we satisfy the boundary matching at r_x and the criterion for truncating the series in Eq. (16) to first order. We mention that a similar alternative method involving inward integration of the TF equation was tried with no particular advantage for the conditions of interest.

V. RESULTS AND DISCUSSION

We present results for the spatial dielectric function, $\bar{\epsilon}(r)$, defined here through[27]

$$\varphi(r) = \frac{Ze}{\bar{\epsilon}(r) r} \ . \quad (32)$$

From Eq. (2a) we have

$$\lim_{r \to 0} \bar{\epsilon}(r) = 1 \ . \quad (33)$$

In view of Eq. (21), which applies for small φ (or large r) and Eq. (32) we find

$$\bar{\epsilon}(r) \approx \frac{Ze}{A} e^{Kr}, \quad r \to \infty \ , \quad (34)$$

i.e., $\bar{\epsilon}(r)$ diverges exponentially for large r. This shows metallic-like screening in the nonzero-T insulator for large r. Note that for zero temperature ($K = 0$) it was earlier found in this TF model that $\bar{\epsilon}(r) = \epsilon_0$ for r larger than some finite distance r_0 where ϵ_0 is a constant[4,5]

Figure 3 presents results for $\bar{\epsilon}$ versus r for zero temperature and for three temperatures of the order of the gap. Parameter values for these plots are $Z = +1$, $E_g = 0.1$ eV, $B = 1.0$ eV, $m_c = 1.0$, $m_v = -1.0$, $d_c = 1.0$, and $d_v = 1.0$. The value for $\bar{\epsilon}$ is seen to go to unity as $r \to 0$ for all cases [Eq. (33)]. For $r \to \infty$ all curves tend to straight lines in the semilog plot. The curve for $T = 0$ saturates to a constant value, $\epsilon_0 \approx 30$, as $r \to \infty$. The curves for $T \neq 0$ are seen to be increasingly above the curve for $T = 0$ with larger T. The asymptotic "linear" behavior (in the semilog plot) of $\bar{\epsilon}(r)$ as $r \to \infty$. for $T \neq 0$ implies exponential

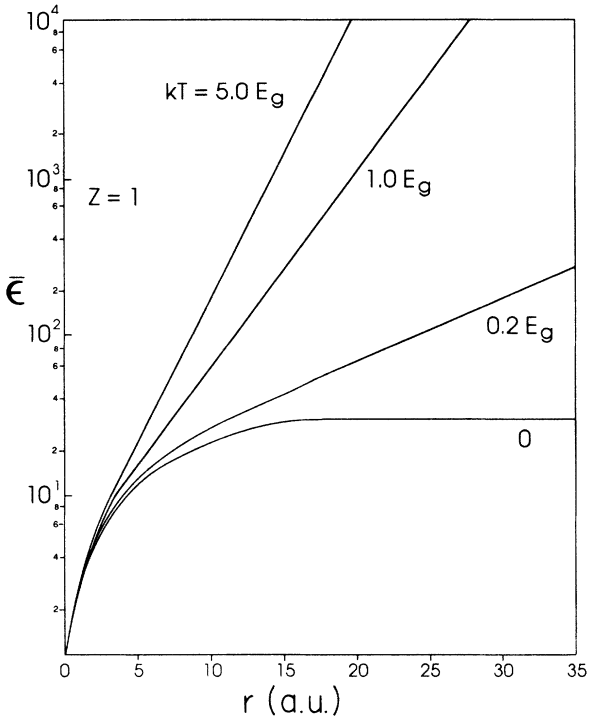

FIG. 3. Spatial dielectric function vs position for several temperatures. (Here $E_g=0.1$ eV, $B=1.0$ eV, $m_c=|m_v|=1.0$ a.u., $d_c=d_v=1.0$.)

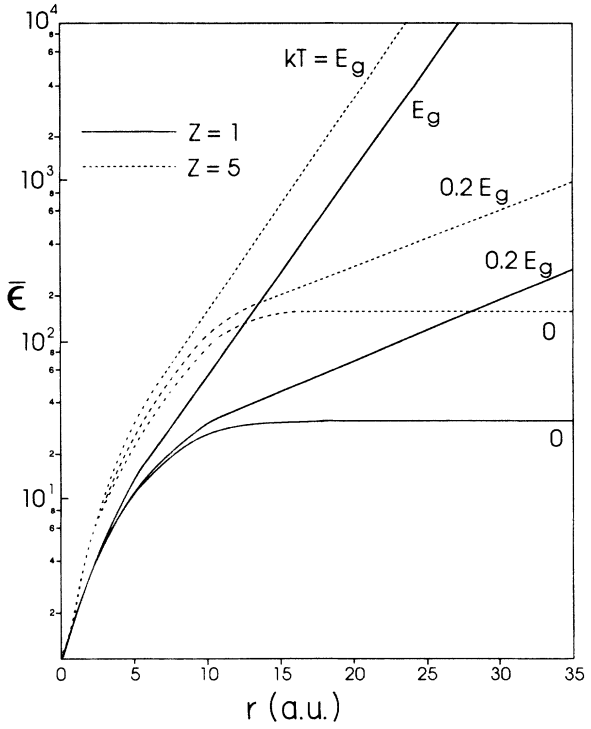

FIG. 4. Spatial dielectric function vs position for three temperatures and showing for each temperature the effect of varying Z. (Here $E_g=0.1$ eV, $B=1.0$ eV, $m_c=|m_v|=1.0$ a.u., $d_c=d_v=1.0$.)

growth in $\bar{\epsilon}(r)$ as anticipated in Eq. (34). Higher T leads to more rapid exponential growth for large r. For the moderate temperatures of interest this is due to the larger number of free carriers at higher T which enhance the metallic-like screening. We can also note that the explicit form of K for low temperatures [Eq. (28)] shows that when β decreases [while still keeping β very large as required by the underlying assumption for Eq. (28)], K indeed increases. We observe that all three $T\neq 0$ curves show a crossover from the $T=0$ behavior to the $T\neq 0$ behavior at ~ 5 a.u. Note also that since $K\rightarrow 0$ as $\beta\rightarrow 0$ (as discussed in Sec. III), the $\bar{\epsilon}(r)$ curve will, for *very* high temperatures, tend to revert to unity (i.e., zero screening). This behavior is not evident in Fig. 3 as our temperatures are moderate, keeping with our practical interests.

We qualitatively anticipate the result of including dielectric polarization effects in calculating $\bar{\epsilon}(r)$. [We assume a spatially varying dielectric constant $\kappa(r)$ which tends to κ_0 for $r\rightarrow\infty$ and to unity for $r\rightarrow 0$.] For large r, we have, replacing K by K_1 in Eq. (34) and using $K_1=K/\kappa_0^{1/2}$ [Eq. (23)], that $\bar{\epsilon}(r)$ will increase less rapidly with r as κ_0 increases. Further, we very roughly estimate the crossover distance r_c for $\bar{\epsilon}(r)$ in going from the small r (quantum) to large r (thermally dominated) regime as $r_c\sim 1/K_1$. Thus, r_c should increase for increasing bulk dielectric constant κ_0. For $r\ll r_c$ we expect that dielectric polarization will have a relatively small effect [$\bar{\epsilon}(r)\rightarrow 1$ as $r\rightarrow 0$].

Figure 4 shows the effect on $\bar{\epsilon}(r)$ of varying Z at several temperatures. Band-structure parameter values here are the same as for Fig. 3. Comparing curves in Fig. 4 at the same temperature shows that the effect of increasing Z is to increase $\epsilon(r)$, a nonlinear effect. The nonlinearity in φ with respect to Z is a consequence of the nonlinearity of the TF equation. This behavior is evident in the results of Adawi.[10] [He considers the extrinsic case (single-carrier band) with an approximate nonlinear TF analysis (see above).] Other authors studying the nonlinear TF equation for this problem have generally set $Z=1$ at the outset making this behavior less apparent in their results. This nonlinear behavior was also seen (using the present TF model) for $T=0$,[4,5] i.e., ϵ_0 (above) was found to be Z dependent.

We note that the larger-r exponentially growing portions of the curves for the same temperature but different Z have the same exponential growth factor K. [The Z independence of K is evident from Eq. (17).] We point out that the nonlinear screening behavior seen here would, of course, still be present if we include dielectric polarization effects.

Figure 5 shows the effect on $\bar{\epsilon}(r)$ due to variation of the gap at three different temperatures. The band-structure parameter values here (other than E_g) are the same as in Fig. 3. In addition, we now consider a negative impurity with $Z=-1$. At $T=0$ the effect of increasing the gap is to decrease $\bar{\epsilon}(r)$, i.e., to decrease the screening effect. This was discussed for the present model earlier.[4,5] Basically as the gap increases we must be closer to the negative impurity in order for the local valence band to have crossed the gap having swept upward in energy upon moving in from infinite distance. This means that the

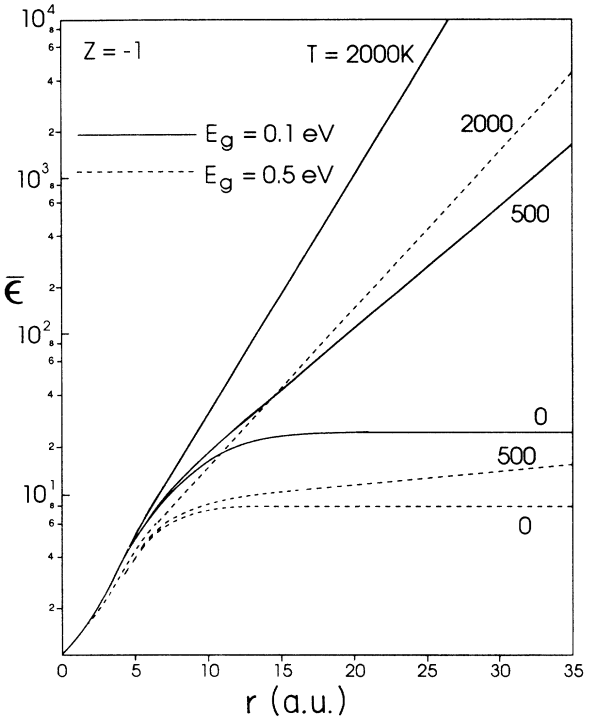

FIG. 5. Spatial dielectric function vs position for three temperatures and showing for each temperature the effect of varying E_g. (Here $B=1.0$ eV, $m_c=|m_v|=1.0$ a.u., $d_c=d_v=1.0$.)

screening cloud is smaller.[28] This "band-shift" effect, as we vary E_g at $T=0$, should carry over to some degree at nonzero temperature (see Fig. 2 for the negative impurity case). In addition (at $T\neq 0$), for a larger gap the thermally induced occupation in the local conduction band and depletion in the local valence band will diminish. Thus, as the gap increases the thermal contribution to the screening will decrease, leaving an overall screening response nearer the $T=0$ form. Thus, including "band-shifting" and thermal effects, we see that a decrease in the screening response for an increase in gap should be present at nonzero temperature (as seen in the results). Notice also from the larger-r exponential regions of the curves, that the K values are different in all $T\neq 0$ cases. This follows from the E_g and T dependence of K [Eq. (17)]. The effect of increasing gap leading to $\bar{\varepsilon}(r)$ being "closer" to the $T=0$ form is particularly evident in the two $T=500$ K curves, one at $E_g=0.1$ eV, the other at $E_g=0.5$ eV. The higher-temperature curves at $T=2000$ K show less of a difference for the same two gaps. This is due to the now increasing importance of the thermal screening relative to the above-mentioned local "band-shifting" effect and to less sensitivity of this thermal screening (at the higher temperature) to the gap increase.

VI. CONCLUSION

We have presented an application of the two-band generalization of the Thomas-Fermi method to electrostatic screening of a point charge in pure insulators and/or semiconductors at nonzero temperatures. As noted, the basic two-band TF approach (within a linearized framework) was utilized earlier by Brooks and Herring[1] and by Dingle[2] in studies of screening of a point charge in a semiconductor (focusing on the extrinsic case; see Sec. I). More recently, this approach was used by the author for the present problem but at zero temperature.[4,5]

A main focus in the present study has been on the effect on the screening response of the excess external charge in the local conduction and valence bands due to the presence of the impurity, background, and remaining electrons in the system. In this initial model study we do not include in the main calculation the effect of dielectric polarization. We do, however, discuss (in some cases quantitatively) some implications of this effect.

We observed that the original fully nonlinear nonzero-temperature TF equation obtained, though not generally soluble in closed form, did admit to an approximate form for the general solution for φ for the case of small φ corresponding to the outer tail region. This was a Yukawa form which evidenced complete metallic screening. In the strictly zero-temperature case we earlier found, using the same TF approach, incomplete nonmetallic screening. The falloff constant K in the exponential of the $T\neq 0$ small φ form was, in general, found to be given in terms of two "Fermi-type" integrals. However, it was evaluated exactly for the case of low temperature. Our results for the spatial dielectric function $\bar{\varepsilon}(r)$ (found by numerical solution of the full TF equation) showed several qualitatively reasonable features. For the moderate range of T considered, $\bar{\varepsilon}(r)$ increased as T increased. We considered the effect on $\bar{\varepsilon}(r)$ of varying Z and E_g at nonzero temperature: In varying Z we found a nonlinear screening response (a consequence of the nonlinearity of the TF equation). Increasing E_g led to a decrease in the screening response as a result of local "band-shifting" effects and a decrease in the thermal excitations. Future work being considered on insulator and/or semiconductor screening response within this model will further examine dielectric polarization effects (as noted) and will examine the effect of exchange.

ACKNOWLEDGMENTS

The author is very appreciative of support for this project through the National Science Foundation (NSF) Grant No. DMR-8704347.

*Permanent address.

[1]H. Brooks, Phys. Rev. **83**, 879 (1951); in *Advances in Electronics and Electron Physics,* edited by L. Marton (Academic, New York, 1955), Vol. 7, p. 85. See also, W. Jones and N. H. March, *Theoretical Solid State Physics* (Wiley-Interscience, London, 1973), p. 988.

[2]R. B. Dingle, Philos. Mag. **46**, 831 (1955).

[3]Here the semiconductors are extrinsic with donors and acceptors concentrated in spatially separated regions. Other systems involving a semiconductor surface can also be analyzed

in a similar way. See, e.g., J. P. McKelvey, *Solid State and Semiconductor Physics* (Harper and Row, New York, 1966), Chaps. 12 and 16.

[4]J. Oliva, Phys. Rev. B **35**, 3431 (1987).

[5]J. Oliva (unpublished).

[6]R. Mansfield, Proc. R. Soc. London, Ser. B **69**, 76 (1956).

[7]P. Csavinszky, Phys. Rev. B **14**, 1649 (1976).

[8]R. Resta, Phys. Rev. B **19**, 3022 (1979).

[9]P. Csavinszky, Philos. Mag. **10**, 231 (1964).

[10]I. Adawi, Philos. Mag. **13**, 331 (1966).

[11]P. Csavinszky, Phys. Rev. **14**, 4483 (1976).

[12]K. R. Brownstein, Phys. Rev. B **22**, 2131 (1980). The variational procedure here applies to the exact (i.e., fully nonlinear) TF equation.

[13]J. R. Meyer, Phys. Rev. B **20**, 1762 (1979).

[14]N. Takimoto, J. Phys. Soc. Jpn. **14**, 1142 (1959).

[15]G. L. Hall, J. Phys. Chem. Solids **23**, 1147 (1962).

[16]F. Stern, Phys. Rev. **158**, 697 (1967).

[17]B. K. Agarwal and Narendra Singh, Phys. Lett. **95A**, 319 (1983).

[18]J. D. Patterson and S. L. Lehoczky, Phys. Lett. A **137**, 137 (1989).

[19]D. Chattopadhyay and H. J. Queisser, Rev. Mod. Phys. **53**, 745 (1981).

[20]The formal results of Dingle (Ref. 2) (in his discussion of the case of carriers in both bands) and Stern (Ref. 16) do directly carry over to the intrinsic case.

[21]In our earlier treatment of the positive impurity case at strictly zero temperature (Ref. 4), the filling level was at $E=0$. In a subsequent study for the negative (and to a lesser extent positive) impurity case (Ref. 5), we used the more physical $T\rightarrow 0$, and thus the filling level was at $E_g/2$.

[22]By dielectric polarization effects we mean charge-density contributions tied in with the induced density of microscopic "dipoles." These would be, roughly speaking, associated with the underlying ion cores and bonds (not directly included in our model). These effects are a further consequence of the underlying (local) periodic potential of the actual crystal at a level beyond that of the simple model local band structure and band-filling picture used here. Dielectric polarization does not, in any case, enter the strong-field region $r\rightarrow 0$. For intermediate r, significant excess charge filling (depletion) in the local conduction (valence) band [for $Z>0$ ($Z<0$)] will still affect the dielectric polarization which for this r range should have an effect on φ. For large r, where φ is small, the dielectric polarization effect will be associated with the usual static bulk dielectric constant κ_0 and would be incorporated in the TF analysis by the replacement: $\nabla^2\rightarrow\kappa_0\nabla^2$ in Eq. (1). Note that where the approximation of neglect of dielectric polarization is valid for $r\rightarrow 0$ but not $r\rightarrow\infty$, the often used approximation $\nabla^2\rightarrow\kappa_0\nabla^2$ in the TF equation for *all* r is valid for $r\rightarrow\infty$ but not $r\rightarrow 0$. Both approximations (but the former more so) give incorrect large-r behavior of φ. (In the latter approximation, this is due to the error in φ at smaller r.)

[23]Spatially varying dielectric functions have been discussed, e.g., (for Si), by M. Azuma and K. Shindo, J. Phys. Soc. Jpn. **19**, 424 (1964) and (for Ge) by S. Okuro and M. Azuma, *ibid.* **20**, 1099 (1964).

[24]N. W. Ashcroft and N. D. Mermin, *Solid State Physics* (Holt, Reinhart, Winston, New York, 1976), Chaps. 28 and 29.

[25]This is the well-known result except for inclusion of the degeneracy-related term here.

[26]The equation in terms of p rather than φ is numerically simpler to handle near the origin [recall $\varphi(r)\sim 1/r$ for $r\rightarrow 0$].

[27]The spatial dielectric function defined here has been used in $T=0$ studies of point-charge screening (see, e.g., R. Resta, Phys. Rev. B **16**, 2717 (1977)).

[28]In this case (at $T=0$), φ is negative; as we move in from infinity the local band structure will sweep upward. The screening cloud (of holes) will extend out to the distance r_0 where the local valence-band maximum is at the Fermi level at the gap midpoint. (For smaller distances the local valence band will be partially or completely depleted; see Ref. 5.) It is found (Ref. 5) that r_0 decreases as the gap increases, i.e., the local valence-band maximum can reach the higher gap midpoint only at a smaller distance from the impurity.